

1 **Thermo-hydraulic Responses of Unsaturated Sand Around a Model Energy Pile**

2

3 **Mohammed Faizal**

4 Research Fellow, Monash University, Department of Civil Engineering, 23 College Walk,
5 Clayton, Vic. 3800, Australia. Telephone: +613 9902 9988; Email:
6 mohammed.faizal@monash.edu

7

8 *** Abdelmalek Bouazza (Corresponding Author)**

9 Professor, Monash University, Department of Civil Engineering, 23 College Walk, Clayton,
10 Vic. 3800, Australia. Telephone: +61 3 9905 4956; Email: malek.bouazza@monash.edu

11

12 **John S. McCartney**

13 Professor and Department Chair, University of California San Diego, Department of Structural
14 Engineering, 9500 Gilman Drive, SME 442J, La Jolla, CA 92093-0085, USA, Telephone:
15 +1 858 534 9630; Email: mccartney@ucsd.edu

16

17

18

19

20

21

22

23

24

25

26

27

28

29 **Abstract**

30 This paper examines the effects of monotonic and cyclic temperature changes of a
31 model energy pile (diameter = 25 mm and length = 264 mm) on the variations in temperature
32 and volumetric water content of surrounding unsaturated sand. Water flowed away from the
33 pile during heating to 36°C and towards the pile during cooling to 5°C, causing soil drying and
34 wetting near the pile, respectively. The change in volumetric water content was time-
35 dependent, non-linear and slower than the change in soil temperature and continued to evolve
36 after the soil temperature changes stabilized. Cyclic heating/cooling induced lower thermo-
37 hydraulic changes in the soil than monotonic heating and cooling. The most significant changes
38 in soil temperatures and volumetric water content were closest to the pile at a radial distance
39 of 20 mm from the edge of the pile and reduced with increasing radial distance for all cases.
40 The largest change in the degree of saturation was near the pile and was up to 6% for monotonic
41 heating. Cyclic heating/cooling induced irreversible cyclic hydraulic responses near the pile
42 with consecutive thermal cycles and caused a permanent reduction in the soil volumetric water
43 content. However, these irreversible cyclic effects were dominant at a radius of 20 mm and
44 reduced with increasing radial distance from the energy pile. The change in volumetric water
45 content was time-dependent, indicating that the ratio of heating to cooling times during cyclic
46 heating/cooling will have a significant effect on the reversibility of hydraulic responses under
47 temperature cycles.

48

49 **Keywords:** *Energy pile; temperature cycles; unsaturated soil; thermo-hydraulic response.*

50

51

52

53

54 **Introduction**

55 The temperatures of energy piles and surrounding soils vary according to the heating
56 and cooling cycles of ground source heat pumps (GSHPs). Any changes in the soil's
57 temperatures caused by the cyclic or monotonic operation of the GSHPs will induce water
58 movement within the soil's pores, particularly for unsaturated soils which are multi-phase
59 porous media. Thermally-induced water flow in unsaturated soils occurs due to the influence
60 of temperature on the changes in properties of the pore water (e.g. density, viscosity, surface
61 tension) and due to evaporation and condensation of pore water (Philip and DeVries 1957;
62 Smits et al. 2013; Başer et al. 2018). The thermo-hydraulic variations of unsaturated soils could
63 potentially affect the piles' thermal and geotechnical performance.

64 The thermal performance of the pile is affected due to an increase or reduction in the
65 soil thermal conductivity when the soil gains or loses water, respectively, which affects the
66 heat transfer between the pile and the ground (e.g. Akrouch et al. 2016; Coccia and McCartney
67 2016; Wang et al. 2016; Başer et al. 2018; Hedayati-Dezfooli and Leong 2019; Sani and Singh
68 2020). The mechanism of heat transfer between the energy pile and the soil (very often
69 unsaturated) is, therefore, a combination of conduction and convection rather than the
70 commonly assumed conduction being the primary mechanism (Wang and Qi 2011; Moradi et
71 al. 2015; Moradi et al. 2016; Başer et al. 2018). Thomas and Rees (2009), Choi et al. (2011)
72 and Akrouch et al. (2016) indicated that the thermal efficiency of energy piles tended to reduce
73 when the soil degree of saturation reduces due to drying.

74 Temperature variations of unsaturated soils affect their thermo-hydro-mechanical
75 behaviour (Uchaipichat and Khalili 2009; McCartney et al. 2014; Coccia and McCartney
76 2016). Changes in the soil thermo-hydro-mechanical behaviour would also affect the coupling
77 between the energy pile and the soil, hence the pile's long-term geotechnical performance.
78 Wang et al. (2015) investigated the shaft capacity of a field-scale energy pile installed in

79 unsaturated sand using Osterberg cells for static load testing. They found that the pile shaft
80 capacity increased after heating. An early centrifuge modelling study by McCartney and
81 Rosenberg (2011) also observed an increase in the ultimate axial capacity of semi-floating
82 energy piles in unsaturated silt with increasing temperature and hypothesised that this was due
83 to an increase in radial stresses due to differential expansion of the pile and soil. However, later
84 centrifuge modelling studies on semi-floating energy piles in unsaturated silt and dry sand by
85 Goode and McCartney (2015) found an increase in ultimate axial capacity was only observed
86 in unsaturated silt. They hypothesised that the increases in axial capacity of energy piles with
87 increasing temperature were caused by an increase in soil effective stress due to drying
88 triggered by the heating process. Behbehani and McCartney (2020) recently analysed
89 unreported dielectric sensor measurements from Goode and McCartney (2015). They found
90 that thermally-induced drying was the cause of the observed increase in axial capacity,
91 confirming the importance of considering the impacts of coupled heat transfer and water flow
92 on energy pile behaviour.

93 Several physical and numerical studies have generally shown that drying occurs in
94 unsaturated soils in the vicinity close to an underground heat source during heating (e.g.
95 Thomas et al. 2001; Wang and Qi 2011; Wang et al. 2012; Goode 2013; Chen et al. 2014;
96 Moradi et al. 2015; Wang et al. 2015; Başer et al. 2016; Coccia and McCartney 2016; Chen et
97 al. 2018; Başer et al. 2018; Jahangir et al. 2018; Cherati and Ghasemi-Fare 2019; Hedayati-
98 Dezfooli and Leong 2019; Başer and McCartney 2020; Gao et al. 2020). Studies conducted on
99 thermo-hydraulic responses of unsaturated soils during monotonic cooling are scarce. A
100 preliminary study conducted on monotonic cooling of a model energy pile in loose unsaturated
101 sand has shown evidence of an increase in volumetric water content near the pile (Cameron et
102 al. 2016).

103 Cyclic temperature variations result from seasonal or daily intermittent operations of
104 the GSHP with either natural or forced ground thermal recoveries (Brandl 2006; Yi et al. 2008;
105 Wood et al. 2010; Dai et al. 2015; Faizal et al. 2016; Murphy and McCartney 2015; McCartney
106 and Murphy 2017; Faizal et al. 2018, 2019a, 2019b). Cyclic temperature changes, particularly
107 for systems with daily forced recharging using solar energy or cooling towers, induce frequent
108 temperature reversals of the pile and the soil (Faizal et al. 2016; Faizal and Bouazza 2018).
109 This would ideally cause frequent hydraulic reversals, and hence, repetitive drying/wetting
110 cycles of the soil which could lead to a complex response of stresses in the soil. The frequent
111 cyclic thermo-hydraulic responses of unsaturated soils around energy piles are not well
112 understood yet. A few physical model studies on cyclic temperature changes of energy piles in
113 unsaturated soils have shown that the changes in the degree of saturation in one thermal cycle
114 tend to recover in the following cycle, but the recovery of the degree of saturation is much
115 lower than the restoration of soil temperatures (Moya et al. 1999; Goode 2013; Stewart and
116 McCartney 2014; Cameron et al. 2016). This was confirmed through simulations of coupled
117 heat transfer and water flow surrounding a geothermal heat exchanger in an unsaturated soil
118 layer by Baser et al. (2018), albeit for relatively high temperatures representative of a heat
119 storage system. Therefore, cyclic heating/cooling has the potential to cause irreversible changes
120 in soil water content and permanent drying or wetting of the soil near the pile. Further studies
121 are required to investigate cyclic thermo-hydraulic responses of unsaturated soils around
122 energy piles under cyclic temperature changes.

123 An assessment of the thermally induced hydraulic responses of unsaturated soils around
124 energy piles under typical monotonic or cyclic temperatures is needed to improve our
125 understanding of this complex coupled heat and mass transfer problem. This paper sheds some
126 light on the above issue; particularly, it examines the thermo-hydraulic responses of an
127 unsaturated soil layer surrounding a model energy pile when subjected to temperature changes

128 typically encountered in practice. The variations in soil temperatures and volumetric water
129 content are physically assessed at different radial distances from the edge of the pile for
130 monotonic heating, monotonic cooling, and cyclic heating/cooling of the energy pile. Although
131 the laboratory-scale tests in this study are not intended to represent a field-scale energy pile,
132 the heat transfer and water flow processes occurring in the laboratory-scale test are the same
133 as those occurring at the field scale, so this study helps understand the range of transient
134 processes that may occur in unsaturated soils close to energy piles. This is particularly
135 important as the soil closest to the energy pile may have the greatest effect on the pile's
136 mechanical response.

137

138 **Experimental Setup and Procedure**

139 The experiments were conducted on a concrete model energy pile embedded in
140 compacted, unsaturated sand. A schematic of the experimental setup is shown in Figure 1. The
141 diameter and length of the energy pile were 25 mm and 264 mm, respectively. The concrete
142 used consisted of 4.5 mm aggregates and water-to-cement ratio of 0.42. The average uniaxial
143 compressive strength of unreinforced cylindrical concrete samples was 45.4 MPa after 35 days
144 of curing. The concrete's thermal conductivity was 2.2 W/mK and was measured using a
145 divided bar apparatus (Barry-Macaulay et al. 2013; Ali et al. 2016). The model pile was not
146 reinforced since this study focused on the soil's thermo-hydraulic response only and not on the
147 thermo-mechanical performance of the pile. The thermo-hydraulic variations of the sand
148 depend on the heat transfer between the energy pile and the sand. A single U-loop heat
149 exchanger made of copper tubing with an outer diameter of 4 mm and a thickness of 0.5 mm
150 was cast in the concrete. The sand was compacted in a container made of 15 mm-thick Perspex
151 and had dimensions of 560 mm (length) x 560 mm (width) x 300 mm (height). The top, bottom
152 and sides of the container were insulated with earthen wool with a thermal resistance of 2

153 m²K/W to prevent the sand from interacting with local environmental conditions (Figure 1c
154 and Figure 1d).

155 The sand was compacted to a dry density of 1300 kg/m³ to allow an easier installation
156 of the sensors. The soil-water retention curve (SWRC) and the sand's grain size distribution are
157 shown in Figure 2. The SWRC was estimated using the grain size distribution, the sand specific
158 gravity of 2.65, and a porosity of 0.51 (e.g. Aubertin et al. 2003). The sand used had a
159 uniformity coefficient of 2.4 and a gradation coefficient of 1.0 and was classified as poorly
160 graded. The sand was hand-mixed at a target initial gravimetric moisture content of 5% and a
161 total mass of 77.05 kg of wet soil. Losses of water due to evaporation during mixing resulted
162 in an average initial gravimetric water content of 4.4% (corresponding to an initial degree of
163 saturation, S_r , of approximately 11.2%) for the monotonic cooling experiment and 4.7%
164 (corresponding to $S_r = 12\%$) for the monotonic heating and cyclic heating/cooling experiments.
165 The initial temperature and volumetric water content of the compacted sand, recorded from the
166 5TM sensors, were approximately 21°C and 0.08 m³/m³, respectively. The compacted sand's
167 thermal conductivity was 1.0 W/mK and was measured using the KD2 Pro thermal needle
168 probe (Barry-Macaulay et al. 2013).

169 The toe of the energy pile was placed on the container's base. The moist sand was
170 compacted around the energy pile in four 45 mm layers using a hand-held mechanical
171 compactor. The embedded depth of the energy pile was thus 180 mm. Each layer of sand was
172 hand-spread evenly in the box and compacted to the desired 45 mm thickness, which was
173 marked on the container's internal walls, ensuring that all the four layers were compacted to
174 the same thickness and density. Each soil layer's gravimetric water content was verified before
175 compaction to ensure consistency between all the layers. The upper surface of each layer of
176 compacted sand was roughened using sandpaper before compacting the next layer to improve

177 contact between the layers. A plastic sheet was placed on the fourth sand layer to prevent direct
178 interaction between the sand and the insulation and minimise moisture losses from the sand.

179 Four 5TM dielectric sensors (Decagon Inc. of Pullman, WA) were installed
180 approximately at mid-height of the soil column to monitor volumetric water content (VWC)
181 and temperatures simultaneously at radial distances, R , of 20 mm, 50 mm, 80 mm, and 110 mm
182 from the edge of the pile (i.e. $R = R_{\text{sensor}} - R_{\text{pile}}$ from the center of the pile) . The sensors were
183 located on planes 90° from each other to minimize interference on the heat transfer and water
184 flow process during the experiments (Figure 1b). The sensors were pushed vertically in the
185 sand after compacting the third sand layer, followed by the fourth layer's compaction to prevent
186 the influence of room environmental conditions on the sensors' responses during experiments.
187 A Decagon EM50 data logger recorded the VWC and temperature continuously from the
188 sensors at 2-minute intervals.

189 The VWC sensors were calibrated against different gravimetric water contents of the
190 sand (i.e. approximately 3%, 5%, 7%, and 9%) at a dry density of 1300 kg/m^3 . The calibration
191 slopes of the four sensors are shown in Figure 3. The moist sand was compacted in a Polyvinyl
192 chloride cylindrical container with an external diameter of 250 mm, a wall thickness of 7 mm
193 and a height of 255 mm. The sand was hand spread evenly in the container and compacted in
194 three 45 mm layers using a hand-held mechanical compactor. The contact between the
195 compacted layers was improved by roughening each layer's upper surface with sandpaper. The
196 sensors were pushed vertically in the sand after compacting the third layer, and the soil
197 temperature and the VWC were recorded using the Decagon EM50 data logger. The average
198 temperature of the compacted sand was approximately 22°C . Similar to the study of Moradi et
199 al. (2016), it was assumed that temperature did not affect the inferred volumetric water content
200 from the dielectric sensors.

201 Two water baths (model: LAUDA ECO RE 620) were used to circulate warm and cold
202 water in the U-loop of the energy pile at set-point temperatures, simulating monotonic heating
203 and cooling, respectively. The cyclic heating/cooling experiment was conducted by heating the
204 energy pile for 24 hours, followed by cooling for 24 hours. The warm and cold water was
205 circulated at approximately 0.6 liters/min through the heat exchange tubing, which
206 corresponded to a Reynolds number of 2957 during cooling to 5°C and 6070 during heating to
207 36°C. These correspond to turbulent flow conditions in the heat exchanger, which is desirable
208 for optimal heat exchange. The inlet and outlet water temperatures at the pile head were
209 recorded using two thermocouples. Two thermocouples were placed on the container's inner
210 edges to monitor boundary thermal effects. The data from the thermocouples were continuously
211 logged using a Pico Technology's USB-TC08 data logger at 5-minute intervals. The heating,
212 cooling, and cyclic heating/cooling experiments were conducted independently of each other
213 by repeating the experimental procedure for each test.

214 Although the experiments were conducted in a temperature-controlled room, there were
215 instances where the temperature was not constant due to technical issues with the room
216 temperature controller. An XC0424 USB Temperature and Humidity Datalogger was used to
217 record the room temperature and humidity during all the experiments. The room air
218 temperatures and the humidity during the experiments are shown in Figure 4. The room
219 temperatures generally remained around 20°C for all experiments, apart from the days where
220 the room temperature controller was unstable. Variations in room humidity were not expected
221 to affect the experimental results since the setup was insulated and the top of the soil column
222 in the container was covered with a plastic sheet.

223

224 **Results and Discussions**

225 The inlet/outlet water and boundary temperatures are shown in Figure 5. The inlet
226 water temperatures were 5°C during cooling (Figure 5a) and 36°C during heating (Figure 5b)
227 and cycled between 5°C and 36°C during the cyclic heating/cooling test (Figure 5c). The outlet
228 water temperatures were approximately 1.5°C higher and lower than inlet temperatures during
229 cooling and heating, respectively. The average soil temperatures at the container boundary
230 changed by 6°C during monotonic cooling (Figure 5a) and by 3°C during monotonic heating
231 and cyclic heating/cooling (Figure 5b and Figure 5c, respectively). However, these boundary
232 temperature changes remained constant for the duration of the experiments. Hence any
233 boundary effects on the results were also constant. The difference in room temperatures slightly
234 affected the boundary soil temperatures on Day 4 of the cooling test and Day 9 of the heating
235 test. There were instances of some data logging issues during the experiments; hence the
236 temperature monitoring on Day 4 of the cyclic experiments was affected for a few hours (Figure
237 5c). The transient temperature changes of the sand, ΔT_{Soil} , the change in volumetric water
238 content of the sand, $\Delta \theta$, and the change in the sand degree of saturation, ΔS_r , at different radial
239 distances from the edge of the model energy pile are shown in Figure 6. The soil temperatures
240 at Day 4 and Day 9 increased by around 1°C for monotonic cooling (Figure 6a) and monotonic
241 heating (Figure 6d), respectively, due to an increase in room temperatures on these two days.
242 The soil temperatures closely followed the trends of the inlet fluid temperatures and reached
243 thermal equilibrium with operating time and remained stable for all experiments. The cyclic
244 temperature changes returned to similar peak values at the end of heating and cooling for a
245 given radial distance (Figure 6g). Cyclic heating/cooling induced slightly lower soil
246 temperature changes than monotonic heating and monotonic cooling due to the frequent
247 temperature reversals of the energy pile. The largest ΔT_{Soil} for all experiments was close to the
248 pile and reduced with increasing radial distance from the pile's edge.

249 Monotonic cooling reduced the ground temperature below the initial conditions
250 temperature and induced negative soil thermal gradients (Figure 6a). Thus, water moved
251 towards the pile during monotonic cooling, causing an increase in $\Delta\theta$ and ΔSr due to wetting
252 of the soil (Figure 6b and Figure 6c). On the other hand, monotonic heating induced positive
253 temperature changes (Figure 6d). Thus, water moved away from the pile and $\Delta\theta$, and ΔSr
254 reduced due to soil drying during monotonic heating (Figure 6e and Figure 6f). The cyclic
255 heating/cooling induced a repetitive drying and wetting process during heating and cooling
256 cycles, respectively, where $\Delta\theta$ and ΔSr shows a cyclic response due to the cyclic nature of soil
257 temperature changes (Figure 6g, Figure 6h and Figure 6i).

258 Unlike ΔT_{Soil} , $\Delta\theta$ and ΔSr varies with operating time for a given experiment and is not
259 stable, i.e. the VWC does not directly follow the trends of inlet fluid temperatures and continues
260 to change when the soil temperatures had stabilized. There is also a time lag in $\Delta\theta$ and ΔSr
261 between different radial distances with the soil closest to the pile at $R = 20$ mm undergoing an
262 earlier change in volumetric water content, followed by $R = 50$ mm, $R = 80$ mm and $R = 110$
263 mm. It is important to note that the VWC changed eventually with time due to the sustainable
264 application of a constant ΔT_{Soil} , even though the change in VWC was slower than soil
265 temperature change. This indicates that the moisture movement at any given radial location
266 depends on the magnitude of the soil temperature change and the duration that temperature
267 change is maintained; longer time with a fixed ΔT_{Soil} will eventually lead to water movement
268 in unsaturated soils.

269 The largest magnitudes of $\Delta\theta$ and ΔSr are closer to the pile at $R = 20$ mm (i.e. closer to
270 the heat source) for all experiments and reduces with increasing radial distance from the edge
271 of the energy pile. The amplitude of $\Delta\theta$ and ΔSr for cyclic heating/cooling also decreases with
272 increasing radial distance from the heat source (Figure 6h and Figure 6i). The $\Delta\theta$ and ΔSr at R
273 $= 20$ mm for cyclic heating/cooling (Figure 6h and Figure 6i) undergoes a progressive

274 reduction with time since heating was the first cycle and the subsequent cooling time was
275 insufficient to return $\Delta\theta$ and ΔS_r to initial conditions, even though ΔT_{Soil} was reversed beyond
276 initial conditions temperatures (Figure 6g). This confirms that the hydraulic response is much
277 slower than temperature response and that the ratio of heating to cooling times has a significant
278 effect on the water movement. Compared to the initial degree of saturation, the ΔS_r increased
279 by approximately 5% for monotonic cooling (Figure 6c), decreased by about 6% for monotonic
280 heating (Figure 6f) and decreased by around 4% for cyclic heating/cooling (Figure 6i) at $R =$
281 20 mm. There are slight differences in $\Delta\theta$ and ΔS_r between monotonic heating and monotonic
282 cooling, particularly at $R = 80$ mm and $R = 100$ mm. This could have occurred due to the
283 differences in temperature-induced properties of the water in the pores, which could have
284 affected convection in the sand. For example, heating could have increased convection due to
285 a larger influence on water density and viscosity compared to cooling. However, further studies
286 on flow visualisation using numerical studies are required to explain this observation.

287 A comparison of the effect of cyclic heating/cooling against monotonic cooling and
288 monotonic heating at a given radial distance is shown in Figure 7. As discussed earlier, heating
289 and cooling induce moisture movement in opposite directions to each other, and $\Delta\theta$ reduces
290 with increasing radial distance. Cyclic heating/cooling causes lower magnitudes of $\Delta\theta$ than
291 monotonic temperature changes. The $\Delta\theta$ during cyclic heating/cooling after $R = 50$ mm are
292 closer to zero, indicating that variations in the VWC remain near initial conditions compared
293 to monotonic heating and monotonic cooling. Therefore, cyclic temperature operations of
294 GSHPs would be useful for long-term operation of energy piles due to lower impacts on the
295 thermo-hydraulic conditions of the surrounding soil. Long-term physical tests with different
296 heating to cooling ratios are needed to confirm this observation since variations in $\Delta\theta$ depend
297 on the period the change in soil temperatures is maintained.

298 It can be also be observed from Figure 7 that the VWC changed earlier at $R = 20$ mm
299 while there was a time lag at other radial distances. An initial increase in $\Delta\theta$ is observed at
300 $R = 80$ mm and $R = 110$ mm before reducing during monotonic heating (Figure 7f and
301 Figure 7h). Similarly, there is an initial reduction in $\Delta\theta$ before increasing during monotonic
302 cooling at $R = 80$ mm and $R = 110$ mm. This could be attributed to mass balance as water
303 moves between different radial distances in unsaturated soils under temperature gradients
304 (Chen et al. 2014; Chen et al. 2018; Cherati and Ghasemi-Fare 2019). For example, as VWC
305 reduces and moves away from near the pile during heating, there is an initial increase in VWC
306 at other radial distances. This initial increase in VWC is why there is a time lag in VWC
307 reduction during heating at farther radial distances. Similarly, opposite movement of water and
308 mass balance occurs during cooling as water moves from farther radial distances towards the
309 energy pile. This hydraulic balance between different radial distances could also be why $\Delta\theta$ is
310 slightly lower at $R = 80$ mm than $R = 110$ mm during cyclic heating/cooling.

311 The thermal and hydraulic radial thermal influence zones are further assessed in
312 Figure 8 by plotting ΔT_{Soil} and $\Delta\theta$ against different radial distances and at different days of
313 operation. Average magnitudes of ΔT_{Soil} and $\Delta\theta$ are shown for cyclic heating/cooling. For a
314 given experiment, the ΔT_{Soil} magnitudes were similar for all the days at a given radial distance
315 (Figure 8a) since the temperatures had stabilized with operating time. The ΔT_{Soil} magnitudes
316 reduced with increasing radial distance for monotonic heating and monotonic cooling, while
317 the average soil temperature changes remained almost constant and close to zero for cyclic
318 heating/cooling. The $\Delta\theta$ magnitudes shown in Figure 8b also reduce with increasing radial
319 distance from the energy pile and has a similar radial influence zone as ΔT_{Soil} . However, the $\Delta\theta$
320 magnitudes for a given experiment increase with the increasing number of days for any given
321 radial distance, and as discussed earlier, occur due to the prolonged time ΔT_{Soil} is maintained.

322 The $\Delta\theta$ magnitudes versus ΔT_{Soil} are plotted in Figure 9 to better assess the temperature-
323 dependent response of $\Delta\theta$. For monotonic heating and monotonic cooling, $\Delta\theta$ reduced and
324 increased, respectively, approximately between $\Delta T_{Soil} = 6^{\circ}\text{C}$ to 11°C at all radial distances,
325 confirming that $\Delta\theta$ can increase/decrease at a constant ΔT_{Soil} , and that $\Delta\theta$ does not have a linear
326 relationship with ΔT_{Soil} . The $\Delta\theta$ magnitudes during cyclic heating/cooling showed different
327 responses at different radial distances. The $\Delta\theta$ magnitudes at $R = 20$ mm showed a cyclic
328 hysteresis with irreversible responses against a stable range of ΔT_{Soil} (Figure 9a), indicating
329 that permanent reduction in volumetric water content occurred. As discussed for Figure 6,
330 heating was the first cycle and the subsequent cooling time was insufficient to return $\Delta\theta$ to
331 initial conditions at $R = 20$ mm in the cyclic heating/cooling test, hence $\Delta\theta$ reduced with
332 consecutive thermal cycles leading to an irreversible response against ΔT_{Soil} . It is also likely
333 that soil drying during heating could have reduced the hydraulic conductivity of the soil which
334 prevented a return of water during cooling (Coccia and McCartney 2016; Başer et al. 2018);
335 this, however, cannot be confirmed from the current results and requires further physical and
336 numerical studies. The $\Delta\theta$ magnitudes during cyclic heating/cooling at other radial distances
337 (Figure 9b, Figure 9c, and Figure 9d) showed insignificant changes with consecutive thermal
338 cycles, indicating that the zone of influence of permanent increase/decrease of $\Delta\theta$ is closer to
339 the pile at $R = 20$ mm and reduces with increasing radial distance.

340

341 **Conclusions**

342 This paper examined the variations in temperatures and volumetric water content of
343 unsaturated sand around a model energy pile (diameter = 25 mm and length = 264 mm) when
344 the pile was subjected to monotonic heating, monotonic cooling, and frequent cyclic
345 heating/cooling. Water moved away from the pile during heating and towards the pile during
346 cooling, causing drying and wetting of the soil, respectively. Cyclic responses of change in the

347 volumetric water content were observed near the pile during cyclic heating/cooling. The change
348 in volumetric water content was non-linear and slower with respect to soil temperature changes.
349 This resulted in permanent drying of the soil closest to the energy pile after several cycles of
350 heating and cooling. Cyclic heating/cooling induced lower changes in soil temperatures and
351 volumetric water content than monotonic heating/cooling and would, therefore, be useful for
352 long-term energy piles operations. The largest changes in soil temperatures and volumetric
353 water content were closer to the energy pile at a radial distance of 20 mm and reduced with
354 increasing radial distance for all cases. The change in volumetric water content did not stabilize
355 with operating time. It continued to evolve even though soil temperatures had stabilized,
356 indicating that soil moisture variations depend on the magnitudes of change in soil temperatures
357 and the duration the temperature change is maintained. The zone of radial thermal influence of
358 temperature changes and change in volumetric water content was similar.

359 The change in volumetric water content near the pile reduced with consecutive thermal
360 cycles. It showed irreversible responses against change in soil temperatures during cyclic
361 heating/cooling, indicating a permanent reduction in volumetric water content near the pile at
362 a radius of 20 mm. However, these irreversible cyclic effects reduced with increasing radial
363 distance from the pile. Since water movement depends on the magnitude and duration of soil
364 temperature change, the ratio of heating to cooling times during cyclic heating/cooling
365 significantly affects the reversibility of hydraulic responses under temperature cycles. This
366 paper's results and conclusions are based on a small-scale model energy pile embedded in an
367 idealised sand layer and controlled boundary conditions. Even though the results present useful
368 insights into sand's thermo-hydraulic behaviour around energy piles, further in-situ tests are
369 still warranted to understand the temperature dependant water movement in the soil under real
370 boundary conditions. Finally, the results presented in this paper are for a single energy pile.

371 Further studies are required to assess the thermo-hydraulic responses of closely spaced energy
372 piles operating in groups where soil temperature changes are expected to be higher.

373

374 **Data Availability Statement**

375 All data, models, and code generated or used during the study appear in the submitted
376 article.

377

378 **Acknowledgements**

379 This research project was supported by the Australian Research Council's Linkage
380 Projects funding scheme (project number LP120200613). The U.S. National Science
381 Foundation grant CMMI-1054190 supported the third author. The support of all the sponsors
382 (Geotechnical Engineering Pty Ltd, Golder Associates Pty Ltd., Geoexchange Australia Pty.
383 Ltd and Brookfield-Multiplex) is gratefully acknowledged. The opinions expressed in this
384 paper are those of the authors alone.

385

386 **References**

- 387 Akrouch, G.A., Sánchez, M., and Briaud, J-L. 2016. "An experimental, analytical and
388 numerical study on the thermal efficiency of energy piles in unsaturated soils." *Comput.*
389 *Geotech.* 71 (Jan): 207-220. <https://doi.org/10.1016/j.compgeo.2015.08.009>
- 390 Ali, M. A., Bouazza, A., Singh, R. M., Gates, W. P., and Rowe, R. K. (2016). "Thermal
391 conductivity of geosynthetic clay liners". *Canadian Geotechnical Journal*, 53(9): 1510-
392 1521. <https://doi.org/10.1139/cgj-2015-0585>
- 393 Aubertin, M., Mbonimpa, M., Bussière, B., and Chapuis, R. P. (2003). "A model to predict the
394 water retention curve from basic geotechnical properties". *Canadian Geotechnical*
395 *Journal*, 40(6), 1104-1122. <https://doi.org/10.1139/t03-054>
- 396 Barry-Macaulay, D., A. Bouazza, R. M. Singh, B.Wang, and P. G. Ranjith. 2013. "Thermal
397 conductivity of soils and rocks from the Melbourne (Australia) region." *Engineering*
398 *Geology*. 164 (Sept): 131–138. <https://doi.org/10.1016/j.enggeo.2013.06.014>.
- 399 Başer, T., Traore, T. and McCartney, J.S. 2016. "Physical modeling of coupled heat transfer
400 and water flow in soil-borehole thermal energy storage systems in the vadose zone." In
401 *Geothermal Energy: An Emerging Resource*. C.B. Dowling, L.J. Florea, and K.
402 Neumann, eds. GSA Books. Boulder, CO. Geological Society of America Special Paper
403 519. 81-93. [https://doi.org/10.1130/2016.2519\(06\)](https://doi.org/10.1130/2016.2519(06))

404 Başer, T., Dong, Y., Moradi, A.M., Lu, N., Smits, K., Ge, S., Tartakovsky, D. and McCartney,
405 J.S. 2018. "Role of nonequilibrium water vapor diffusion in thermal energy storage
406 systems in the vadose zone". *J. Geotech. Geoenviron. Eng.* 144 (7): 04018038.
407 [https://doi.org/10.1061/\(ASCE\)GT.1943-5606.0001910](https://doi.org/10.1061/(ASCE)GT.1943-5606.0001910)

408 Başer, T. and McCartney., J.S. 2020. "Transient evaluation of a soil-borehole thermal energy
409 storage system". *Ren. Energy* 147 (Mar): 2582–2598.
410 <https://doi.org/10.1016/j.renene.2018.11.012>

411 Behbehani, F. and McCartney, J.S. 2020. "Impacts of unsaturated conditions on the ultimate
412 capacity of energy piles." EUUnsat 2020: The 4th European Conference on Unsaturated
413 Soils. Lisbon, Portugal. Jun. 24-26. E3S Web of Conferences 195, 04005 pp. 1-6.

414 Brandl, H. 2006. "Energy foundations and other thermo-active ground structures." *Géotechnique* 56 (2): 81 – 122. <https://doi.org/10.1680/geot.2006.56.2.81>

416 Cameron, M.D., Faizal, M. and Bouazza, A. 2016. "Soil temperature and moisture variation
417 for the different operating modes of a model energy pile". In *Proc. Geo-Chicago 2016*,
418 758-766. Reston, VA: ASCE. <https://doi.org/10.1061/9780784480168.074>

419 Chen, H., Ding, H., Liu, S., Chen, X., Wu, W. and Wang, Q. 2014. "Experimental study on
420 heat and moisture transfer in soil during soil heat charging for solar-soil source heat
421 pump compound system". *Appl. Therm. Eng.* 70 (1): 1018-1024.
422 <https://doi.org/10.1016/j.applthermaleng.2014.06.030>

423 Chen, H., Chu, S., Luan, D., Li, Q., Zhang, L. and Zhai, H. 2018. "Performance study on heat
424 and moisture transfer in soil heat charging". *Int. J. Sustain. Energy* 37 (7): 669-683.
425 <https://doi.org/10.1080/14786451.2017.1323898>

426 Cherati, D.Y. and Ghasemi-Fare, O. 2019. "Analysing transient heat and moisture transport
427 surrounding a heat source in unsaturated porous media using the Green's
428 function". *Geothermics* 81 (Sep): 224-234.
429 <https://doi.org/10.1016/j.geothermics.2019.04.012>

430 Choi, J.C., Lee, S.R. and Lee, D.S. 2011. "Numerical simulation of vertical ground heat
431 exchangers: intermittent operation in unsaturated soil conditions". *Comput.
432 Geotech.* 38 (8): 949-958. <https://doi.org/10.1016/j.compgeo.2011.07.004>

433 Coccia, C.J. and McCartney, J.S. 2016. "Impact of long-term temperature cycling on the
434 thermo-hydro-mechanical behavior of unsaturated soils surrounding an energy pile."
435 In *Proc. Geo-Chicago 2016*, 42-51. Reston, VA: ASCE.
436 <https://doi.org/10.1061/9780784480137.005>

437 Dai, L., Li, S., DuanMu, L., Li, X., Shang, Y. and Dong, M. 2015. "Experimental performance
438 analysis of a solar assisted ground source heat pump system under different heating
439 operation modes." *Appl. Therm. Eng.* 75 (Jan): 325-333.
440 <https://doi.org/10.1016/j.applthermaleng.2014.09.061>

441 Faizal, M. and Bouazza, A. 2018. "Energy utilisation and ground temperature distribution of a
442 field scale energy pile under monotonic and cyclic temperature changes". In
443 *Proceedings of China-Europe Conference on Geotechnical Engineering*, Vienna,
444 Austria. Edited by W. Wu and H.-S. Yu . Springer Nature, Switzerland, pp. 1591–1594.
445 https://doi.org/10.1007/978-3-319-97115-5_151

446 Faizal, M., Bouazza, A. and Singh, R. M. 2016. "An experimental investigation of the influence
447 of intermittent and continuous operating modes on the thermal behaviour of a full scale

448 geothermal energy pile." *Geomech. Energy Environ.* 8 (Dec): 8 – 29.
449 <https://doi.org/10.1016/j.gete.2016.08.001>

450 Faizal, M., Bouazza, A., Haberfield, C. and McCartney, J.S. 2018. "Axial and radial thermal
451 responses of a field-scale energy pile under monotonic and cyclic temperature
452 changes". *J. Geotech. Geoenviron. Eng.* 144 (10): 04018072.
453 [https://doi.org/10.1061/\(ASCE\)GT.1943-5606.0001952](https://doi.org/10.1061/(ASCE)GT.1943-5606.0001952)

454 Faizal, M., Bouazza, A., McCartney, J.S. and Haberfield, C. 2019a. "Effects of cyclic
455 temperature variations on the thermal response of an energy pile under a residential
456 building". *J. Geotech. Geoenviron. Eng.* 145 (10): 04019066.
457 [https://doi.org/10.1061/\(ASCE\)GT.1943-5606.0002147](https://doi.org/10.1061/(ASCE)GT.1943-5606.0002147)

458 Faizal, M., Bouazza, A., McCartney, J. S., & Haberfield, C. 2019b. Axial and radial thermal
459 responses of energy pile under six storey residential building. *Canadian Geotechnical*
460 *Journal*, 56(7), 1019-1033.

461 Gao, Y., Dong, S., Wang, C., Chen, Y. and Hu, W. 2020. "Effect of thermal intensity and initial
462 moisture content on heat and moisture transfer in unsaturated soil". *Sustain. Cities*
463 *Soc.* 55 (Apr):102069. <https://doi.org/10.1016/j.scs.2020.102069>

464 Goode, J. C., III. (2013). Centrifuge modeling of the thermo-mechanical response of energy foundations.
465 M.S. thesis, Univ. of Colorado, Boulder, CO.

466 Goode, J. C., and J. S. McCartney. 2015. "Centrifuge modeling of end restraint effects in
467 energy foundations." *J. Geotech. Geoenviron. Eng.* 141 (8): 04015034.
468 [https://doi.org/10.1061/\(ASCE\)GT.1943-5606.0001333](https://doi.org/10.1061/(ASCE)GT.1943-5606.0001333)

469 Hedayati-Dezfooli, M. and Leong, W.H. 2019. "An experimental study of coupled heat and
470 moisture transfer in soils at high temperature conditions for a medium coarse soil". *Int.*
471 *J. Heat Mass Tran.* 137 (Jul): 372-389.
472 <https://doi.org/10.1016/j.ijheatmasstransfer.2019.03.131>

473 Jahangir, M.H., Sarrafha, H. and Kasaeian, A. 2018. "Numerical modeling of energy transfer
474 in underground borehole heat exchanger within unsaturated soil". *Appl. Therm.*
475 *Eng.* 132 (Mar): 697-707. <https://doi.org/10.1016/j.applthermaleng.2018.01.020>

476 McCartney, J.S., Coccia, C.J.R., Alsharif, N.A., Stewart, M.A., Baser, T., Traore, T. and Goode
477 III, J.C. 2014. "Unsaturated soil mechanics in geothermal energy applications". In
478 *Unsaturated Soils: Research & Applications*, Khalili, N., A. Russell, A. Khoshghalb:
479 CRC Press, 835-842.

480 McCartney, J.S. and Murphy, K.D. 2017. "Investigation of potential dragdown/uplift effects
481 on energy piles." *Geomech. Energy Environ.* 10 (Jun): 21 – 28.
482 <https://doi.org/10.1016/j.gete.2017.03.001>

483 McCartney, J. S., and J. E. Rosenberg. 2011. "Impact of heat exchange on side shear in thermo-
484 active foundations." In *Proc. Geo-Frontiers 2011*, 488–498. Reston, VA: ASCE.
485 [https://doi.org/10.1061/41165\(397\)51](https://doi.org/10.1061/41165(397)51)

486 Moradi, A., Smits, K.M., Massey, J., Cihan, A. and McCartney, J. 2015. "Impact of coupled
487 heat transfer and water flow on soil borehole thermal energy storage (SBTES) systems:
488 experimental and modeling investigation". *Geothermics* 57 (Sep): 56-72.
489 <https://doi.org/10.1016/j.geothermics.2015.05.007>

- 490 Moradi, A., Smits, K.M., Lu, N. and McCartney, J.S. 2016. "Heat transfer in unsaturated soil
491 with application to borehole thermal energy storage". *Vadose Zone J.* 15 (10):
492 vj2016.03.0027. <https://doi.org/10.2136/vzj2016.03.0027>
- 493 Moya, R.E.S., Prata, A.T. and Neto, J.C. 1999. "Experimental analysis of unsteady heat and
494 moisture transfer around a heated cylinder buried into a porous medium". *Int. J. Heat
495 Mass Tran.* 42 (12): 2187-2198. [https://doi.org/10.1016/S0017-9310\(98\)00322-6](https://doi.org/10.1016/S0017-9310(98)00322-6)
- 496 Murphy, K. D., and J. S. McCartney. 2015. "Seasonal response of energy foundations during
497 building operation." *Geotech. Geol. Eng.* 33 (2): 343–356.
498 <https://doi.org/10.1007/s10706-014-9802-3>
- 499 Philip, J. R., and D. A. de Vries. 1957. "Moisture movement in porous materials under
500 temperature gradients." *Trans. Am. Geophys. Union* 38 (2): 222–232.
501 <https://doi.org/10.1029/TR038i002p00222>.
- 502 Sani, A.K. and Singh, R.M. 2020. "Response of unsaturated soils to heating of geothermal
503 energy pile". *Ren. Energy* 147 (Mar): 2618-2632.
504 <https://doi.org/10.1016/j.renene.2018.11.032>
- 505 Smits, K. M., S. Sakaki, S. E. Howington, J. F. Peters, and T. H. Illangasekare. 2013.
506 "Temperature dependence of thermal properties of sands across a wide range of
507 temperatures (30–70 °C)." *Vadose Zone J.* 21 (1): 1–8.
508 <https://doi.org/10.2136/vzj2012.0033>.
- 509 Stewart, M.A. and McCartney, J.S. 2014. "Centrifuge modeling of soil-structure interaction in
510 energy foundations". *J. Geotech. Geoenviron.* 140 (4): 04013044.
511 [https://doi.org/10.1061/\(ASCE\)GT.1943-5606.0001061](https://doi.org/10.1061/(ASCE)GT.1943-5606.0001061)
- 512 Thomas, H.R. and Rees, S.W. 2009. "Measured and simulated heat transfer to foundation
513 soils". *Géotechnique* 59 (4): 365-375. <https://doi.org/10.1680/geot.2008.59.4.365>
- 514 Thomas H.R., Sansom M., and Rees S.W. 2001. "Non-Isothermal Flow". In: Schrefler B.A.
515 (eds) Environmental Geomechanics. International Centre for Mechanical Sciences
516 (Courses and Lectures), vol 417. Springer, Vienna. https://doi.org/10.1007/978-3-7091-2592-2_3
- 517
- 518 Uchaipichat, A. and Khalili, N. 2009. "Experimental investigation of thermo-hydro-
519 mechanical behaviour of an unsaturated silt". *Géotechnique* 59 (4): 339-353.
520 <https://doi.org/10.1680/geot.2009.59.4.339>
- 521 Wang, B., A. Bouazza, R. Singh, C. Haberfield, D. Barry-Macaulay, and S. Baycan. 2015.
522 "Posttemperature effects on shaft capacity of a full-scale geothermal energy pile." *J.
523 Geotech. Geoenviron. Eng.* 141 (4): 04014125.
524 [https://doi.org/10.1061/\(ASCE\)GT.1943-5606.0001266](https://doi.org/10.1061/(ASCE)GT.1943-5606.0001266).
- 525 Wang, B., Bouazza, A., Barry-Macaulay, D., Singh, M.R., Webster, M., Haberfield, C.,
526 Chapman, G. and Baycan, S. 2012. "Field and laboratory investigation of a heat
527 exchanger pile". In *Proc. GeoCongress 2012* 4396-4405. Reston, VA: ASCE.
528 <https://doi.org/10.1061/9780784412121.452>
- 529 Wang, H. and Qi, C. 2011. "A laboratory experimental study of high-temperature thermal
530 storage in the unsaturated soil using a vertical borehole heat exchanger". *Int. J. Low-
531 Carbon Technol.* 6 (3): 187-192. <https://doi.org/10.1093/ijlct/ctr006>
- 532 Wang, W., Regueiro, R.A. and McCartney, J.S. 2015. "Coupled axisymmetric thermo-poro-
533 mechanical finite element analysis of energy foundation centrifuge experiments in

- 534 partially saturated silt”. *Geotech. Geol. Eng.* 33: 373-388.
535 <https://doi.org/10.1007/s10706-014-9801-4>
- 536 Wang, Z., Wang, F., Ma, Z., Wang, X. and Wu, X. 2016. “Research of heat and moisture
537 transfer influence on the characteristics of the ground heat pump exchangers in
538 unsaturated soil”. *Energ.Buildings* 130 (Oct): 140-149.
539 <https://doi.org/10.1016/j.enbuild.2016.08.043>
- 540 Wood, C.J., Liu, H. and Riffat S.B. 2010. “Comparison of a modelled and field tested piled
541 ground heat exchanger system for a residential building and the simulated effect of
542 assisted ground heat recharge”. *Int. J. Low-Carbon Technol.* 5 (3): 137 – 143.
543 <https://doi.org/10.1093/ijlct/ctq015>
- 544 Yi, M., Hongxing, Y. and Zhaohong, F. 2008. “Study on hybrid ground-coupled heat pump
545 systems.” *Energ. Buildings* 40 (11): 2028–2036.
546 <https://doi.org/10.1016/j.enbuild.2008.05.010>

List of Figures

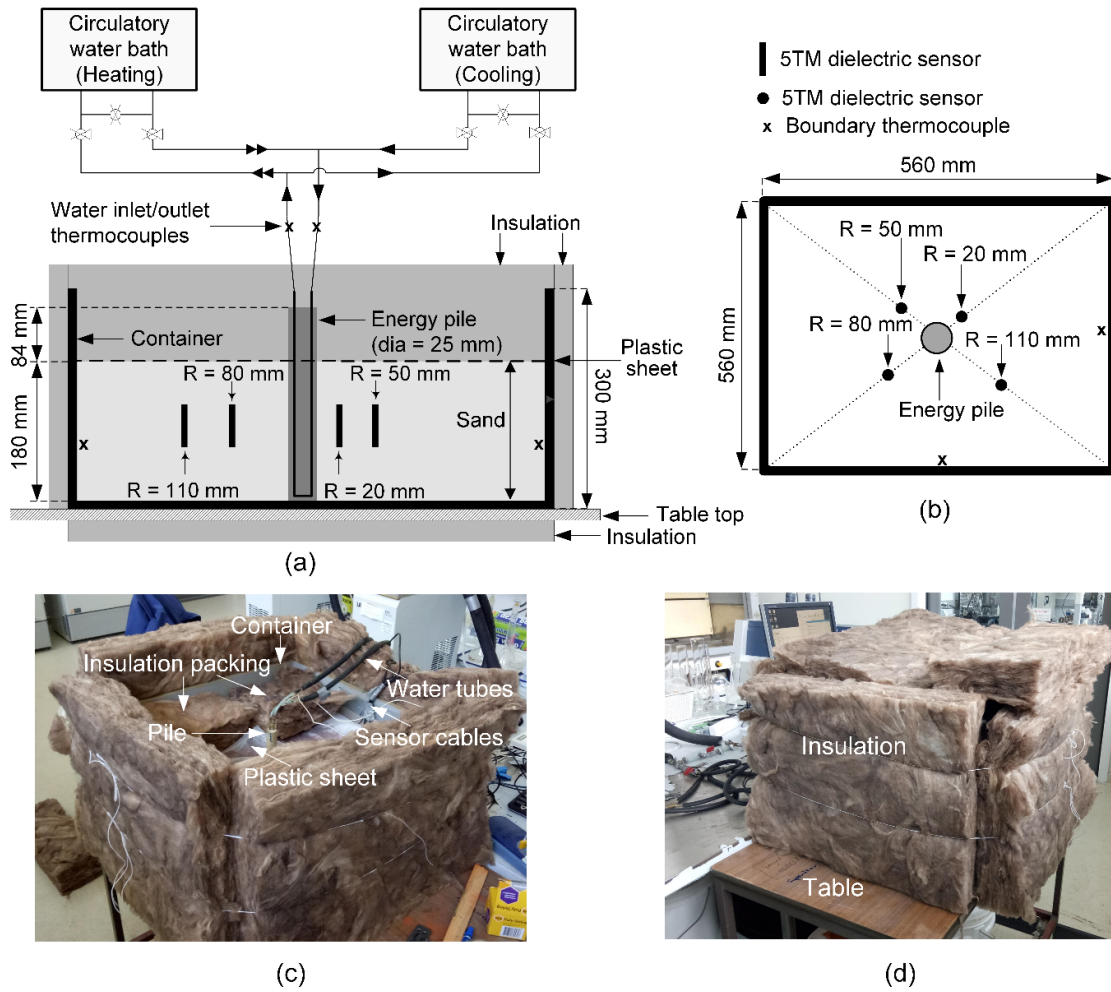


Figure 1. Experimental setup : (a) cross-sectional elevation view; (b) cross-sectional plan view; (c) partially insulated; and (d) fully insulated.

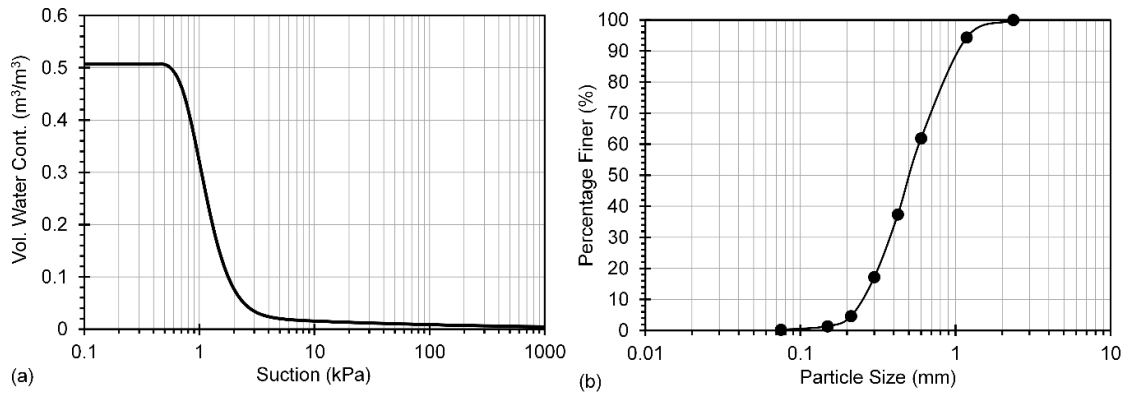


Figure 2. (a) Soil water retention curve; and (b) particle size distribution.

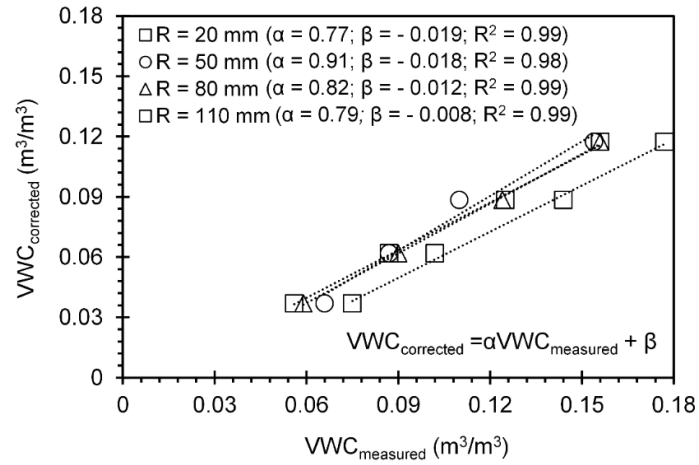


Figure 3. Volumetric water content inferred from the dielectric sensors ($VWC_{measured}$) used at the four radial locations, R , in the experimental setup versus the volumetric water content obtained from oven drying ($VWC_{corrected}$).

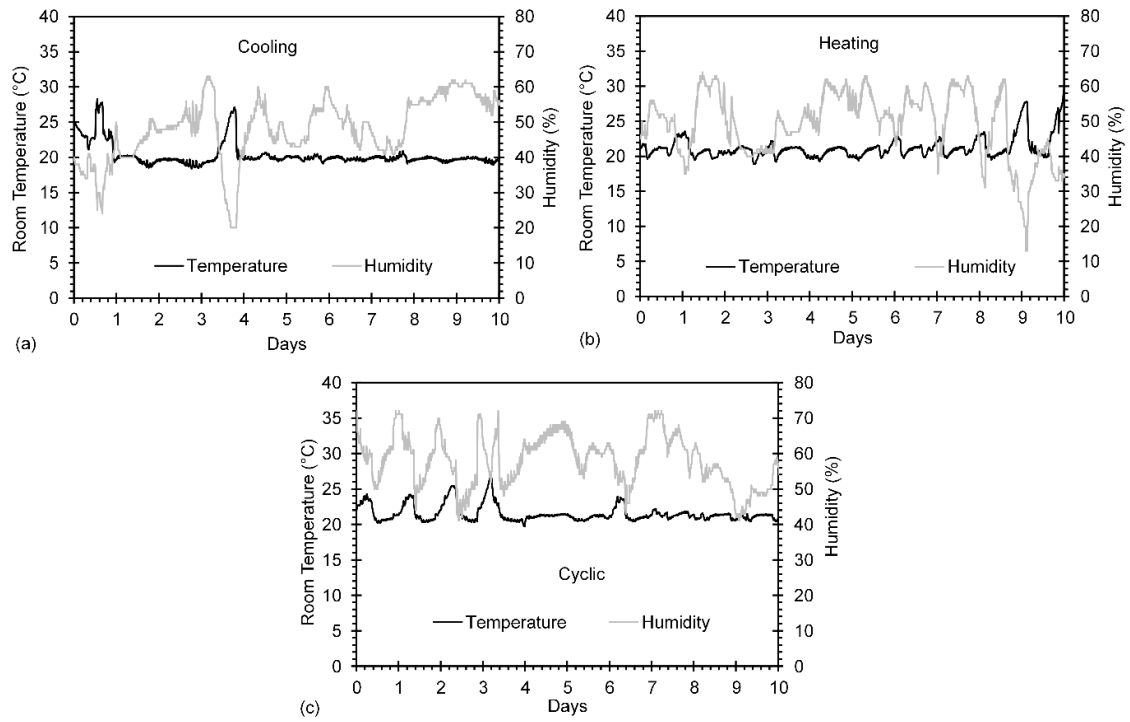


Figure 4. Room temperature and humidity during experiments: (a) cooling test; (b) heating test; and (c) cyclic heating/cooling test.

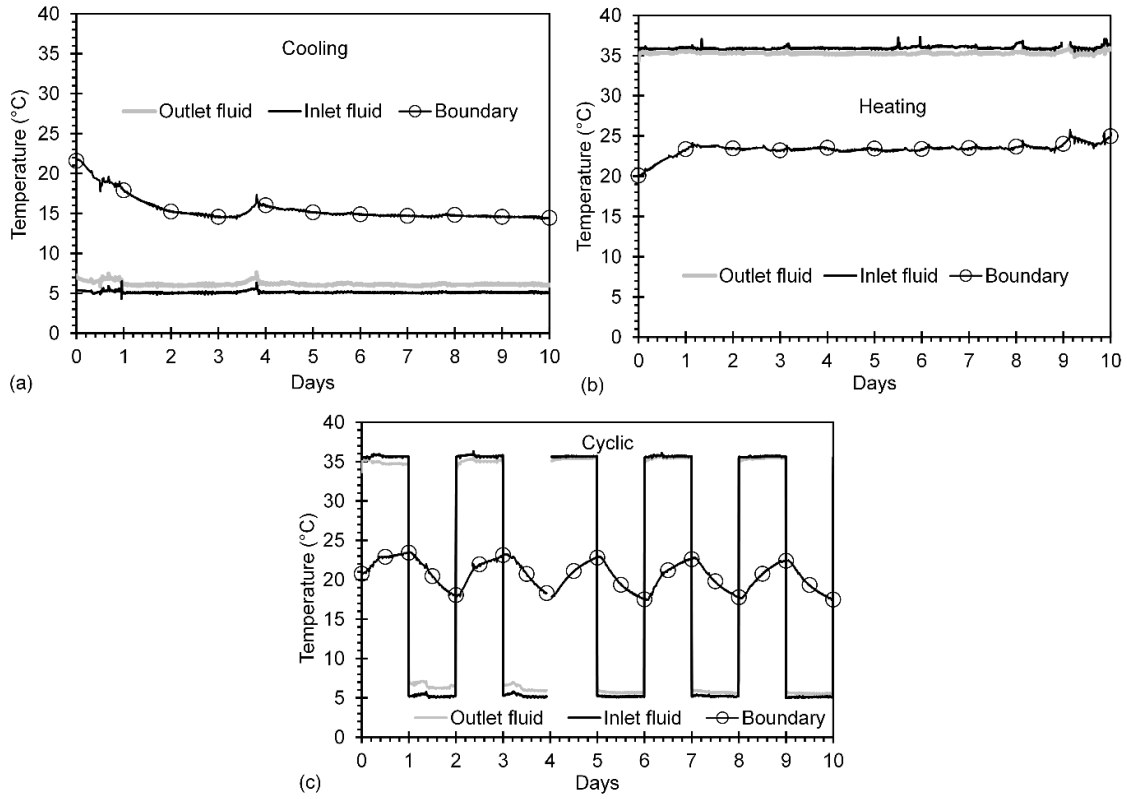


Figure 5. Fluid (water) and boundary temperatures: (a) cooling test; (b) heating test; and (c) cyclic heating/cooling test.

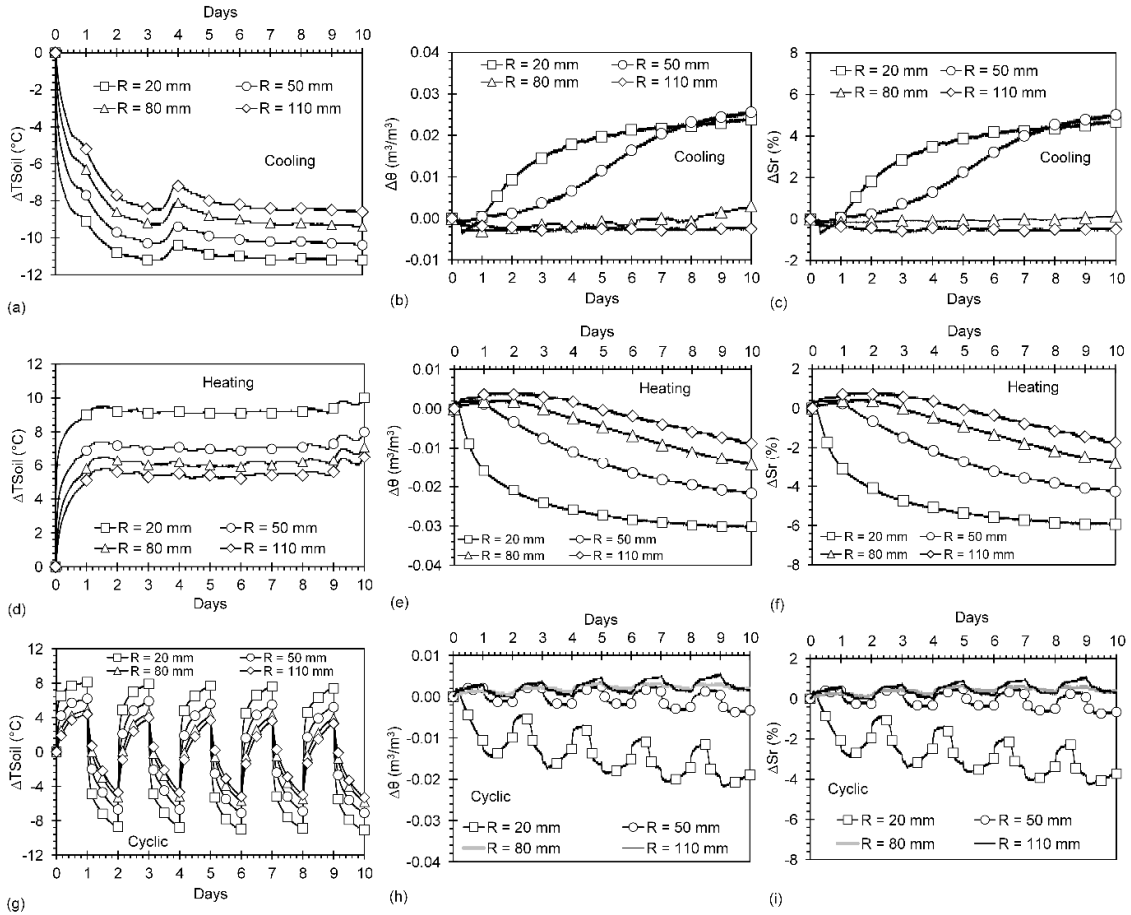


Figure 6. Change in soil temperatures (ΔT_{Soil}), change in soil volumetric water content ($\Delta\theta$), and change in degree of saturation (ΔSr), at different radial locations: (a), (b) and (c) ΔT_{Soil} , $\Delta\theta$, and ΔSr for cooling test, respectively; (d), (e) and (f) ΔT_{Soil} , $\Delta\theta$, and ΔSr for heating test, respectively; and (g), (h) and (i) ΔT_{Soil} , $\Delta\theta$, and ΔSr for cyclic heating/cooling test, respectively.

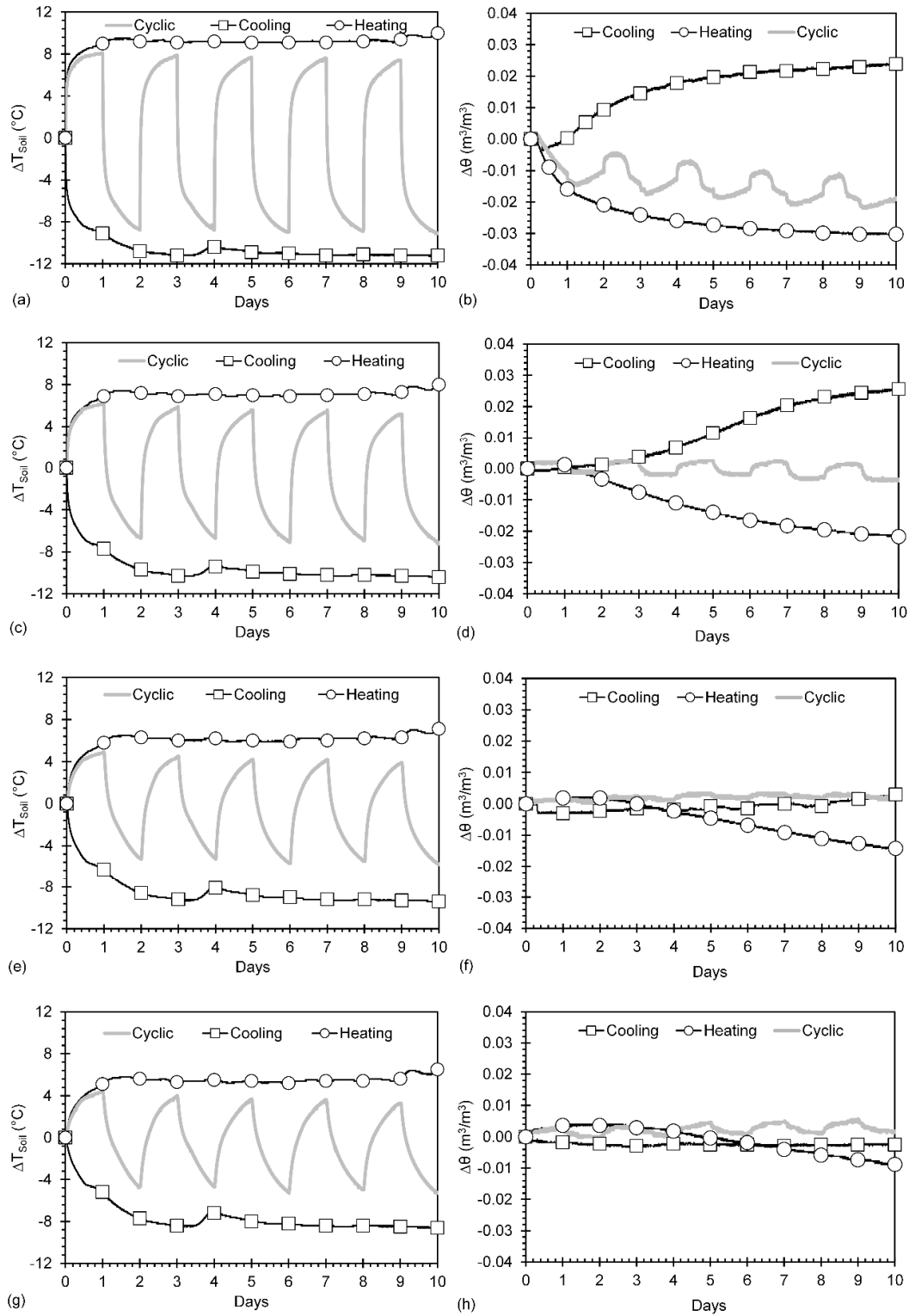


Figure 7. Comparison of ΔT_{Soil} and $\Delta \theta$ for monotonic and cyclic temperature changes of the soil at given radial distances, R : (a) and (b) ΔT_{Soil} and $\Delta \theta$ at $R = 20$ mm, respectively; (c) and (d) ΔT_{Soil} and $\Delta \theta$ at $R = 50$ mm, respectively; (e) and (f) ΔT_{Soil} and $\Delta \theta$ at $R = 80$ mm respectively; and (g) and (h) ΔT_{Soil} and $\Delta \theta$ at $R = 110$ mm, respectively.

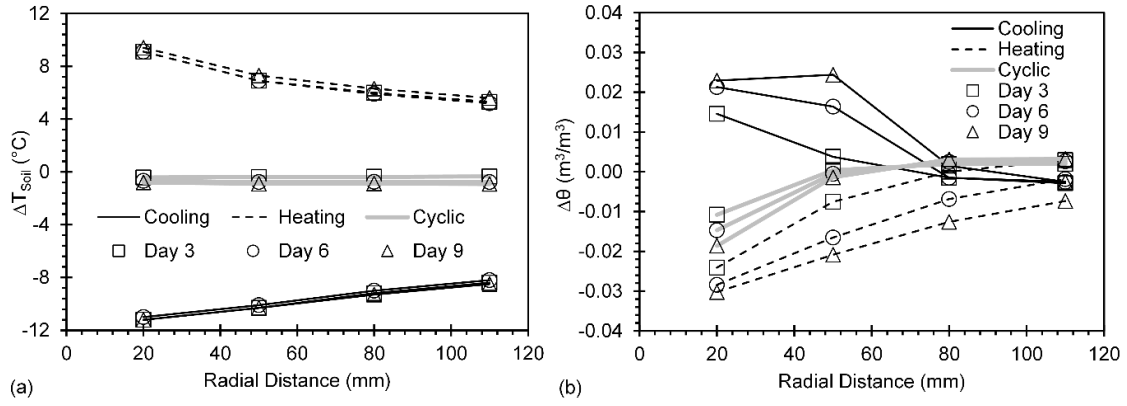


Figure 8. Thermal and hydraulic radial influence zones: (a) change in soil temperatures (ΔT_{Soil}); and (b) change in soil volumetric water content ($\Delta\theta$).

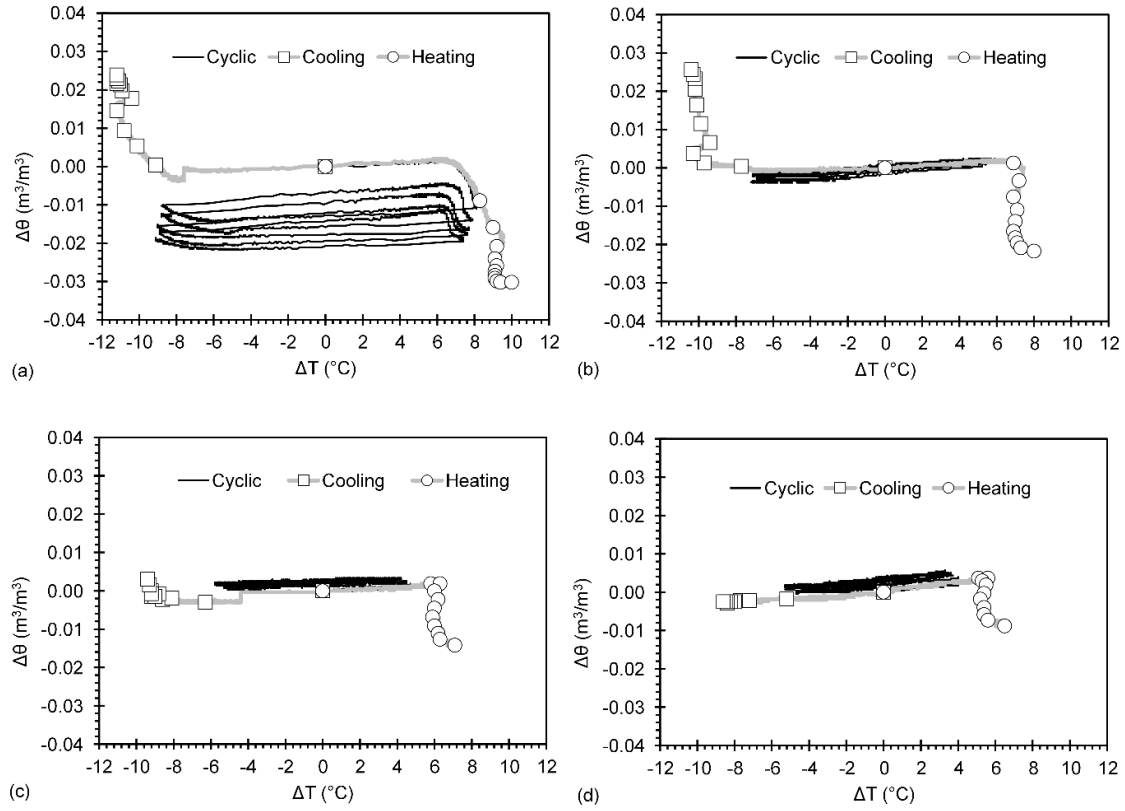


Figure 9. Change in volumetric water content ($\Delta\theta$) plotted against change in soil temperature (ΔT_{Soil}): (a) $R = 20$ mm; (b) $R = 50$ mm; (c) $R = 80$ mm; and (d) $R = 110$ mm.